



Molecular Crystals and Liquid Crystals Science and Technology. Section A. Molecular Crystals and Liquid Crystals

Publication details, including instructions for authors and subscription information:

<http://www.tandfonline.com/loi/gmcl19>

Molecular Antiferromagnets Based on TTF-TYPE Radical Ion Salts

Akira Miyazaki^a, Miki Enomoto^a, Masaya Enomoto^a, Toshiaki Enoki^a & Gunzi Saito^b

^a Department of Chemistry, Tokyo Institute of Technology, Ookayama, Meguro-ku, Tokyo, 152, Japan

^b Department of Chemistry, Kyoto University, Sakyo-ku, Kyoto, 606, Japan

Version of record first published: 04 Oct 2006

To cite this article: Akira Miyazaki, Miki Enomoto, Masaya Enomoto, Toshiaki Enoki & Gunzi Saito (1997): Molecular Antiferromagnets Based on TTF-TYPE Radical Ion Salts, Molecular Crystals and Liquid Crystals Science and Technology. Section A. Molecular Crystals and Liquid Crystals, 305:1, 425-434

To link to this article: <http://dx.doi.org/10.1080/10587259708045077>

PLEASE SCROLL DOWN FOR ARTICLE

Full terms and conditions of use: <http://www.tandfonline.com/page/terms-and-conditions>

This article may be used for research, teaching, and private study purposes. Any substantial or systematic reproduction, redistribution, reselling, loan, sub-licensing, systematic supply, or distribution in any form to anyone is expressly forbidden.

The publisher does not give any warranty express or implied or make any representation that the contents will be complete or accurate or up to date. The accuracy of any instructions, formulae, and drug doses should be independently verified with primary sources. The publisher shall not be liable for any loss, actions, claims, proceedings, demand, or costs or damages whatsoever or howsoever caused arising directly or indirectly in connection with or arising out of the use of this material.

MOLECULAR ANTIFERROMAGNETS BASED ON TTF-TYPE RADICAL ION SALTS

AKIRA MIYAZAKI, MIKI ENOMOTO, MASAYA ENOMOTO and
TOSHIKI ENOKI

Department of Chemistry, Tokyo Institute of Technology, Ookayama, Meguro-ku
Tokyo 152 Japan

GUNZI SAITO

Department of Chemistry, Kyoto University, Sakyo-ku, Kyoto 606 Japan

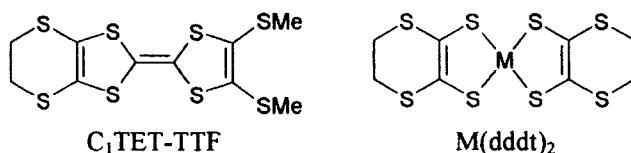
Abstract. We investigate the structure and the magnetic properties of the radical ion salts of C₇TET-TTF and M(ddd_t)₂ (M = Ni, Pt, Au) with FeX₄[−] (X = Cl, Br) anion. Despite the isolated, chain or sheet structure of the magnetic anion within these salts, the magnetic susceptibility shows the three dimensional behavior for all of these salts. This is regarded as a consequence of the coexistence of Fe-X···X-Fe and Fe-X···(donor)_n···X-Fe exchange paths, the latter of which exchange is mediated by the π -electrons on the donor molecules. These salts show the antiferromagnetic transition around liquid helium temperature if FeBr₄[−] is adopted as a counter anion, and their transition temperature is also affected by the central atom (M) substitution. These sensibility can be qualitatively understood as the difference in the magnitudes of the MO coefficients on the halogen and the sulfur atoms at the Fe-X···(donor)_n contacts.

INTRODUCTION

The most striking feature of molecular conductors is the low-dimensionality of their electronic system made of the π -electrons on the molecules. When the magnetic ions, such as transition metal complexes, are incorporated as a counter ion into the conductive radical ion salts, the spins of localized *d*-electrons are expected to interact through the π -electrons on the conduction paths, whose mechanism depends on the transport properties of the salts. If the salt shows metallic behavior, the indirect interaction *via* conduction electrons will be realized. For the insulator case, the magnetic moments will interact through the exchange paths via the localized π -electrons on the donor molecules.

Based on these principles, several salts based on BEDT-TTF (bis(ethylenedithio)-tetrathiafulvalene) have been thus far prepared, most of which have, however, little interaction between the magnetic anions.¹ One of the most noteworthy exception is (BEDT-TTF)₃CuBr₄,² where $s = 1/2$ spins on CuBr₄^{2−} anions interact through close

Br...S contacts ($d_{\text{Br}\cdots\text{S}} = 3.699\text{\AA}$) with donors, and this interaction causes an strong antiferromagnetic interaction $J = -17\text{K}$. This example shows the importance of the close contacts between the chalcogen atom on donor molecule and the halogen atoms on counter anion to realize the desired π - d system.



In this study we have adopted³ $\text{C}_1\text{TET-TTF}$ and M(dddT)_2 ($\text{M} = \text{Ni}, \text{Pt}, \text{Au}$) as good candidates to realize the donor-anion contacts for the following reasons. The $\text{C}_1\text{TET-TTF}$ molecule has two flexible thiomethyl groups, which enable to interact with counter anions by making use of the sulfur's unshared electron pairs elongated along the long axis of the molecule. For M(dddT)_2 system, the electrons in the frontier orbitals are more delocalized to the outer sulfur atoms than those of BEDT-TTF ,⁴ hence the stronger exchange interaction between the donor and the anion will be realized. As magnetic counter anions we used monovalent FeX_4^- ($\text{X} = \text{Cl}, \text{Br}$) for the convenience of the preparation of the salts. Furthermore, the resulted salts tend to be isostructural if the anion is replaced to diamagnetic GaX_4^- anion,⁵ which fact is useful to clarify the role of π -spins on the donor in these systems. We have prepared radical ion salts using these components and, throughout the investigation of the crystal structure, transport properties and magnetic properties, examined the possibility of the π - d interaction on these materials.

EXPERIMENTAL

$\text{C}_1\text{TET-TTF}$ ⁶ and M(dddT)_2 ($\text{M} = \text{Ni}, \text{Pt}, \text{Au}$)^{7,8} were prepared according to the literatures. Elongated plates of samples were grown with galvanostatic anodic oxidation of the donors, using $n\text{-Bu}_4\text{N}^+\text{M}'\text{X}_4^-$ ($\text{M}' = \text{Fe}, \text{Ga}; \text{X} = \text{Cl}, \text{Br}$) as a supporting electrolyte, ethanol ($\text{C}_1\text{TET-TTF}$) or chlorobenzene (M(dddT)_2) as a solvent.

The crystal structure are determined by single crystal X-ray diffraction method with *Rigaku* AFC-7 four-circle diffractometer. Structure were solved using direct methods (*SHELXS-86*),⁹ then refined with full-matrix least-squares method (*SHELXL-93*).¹⁰ DC electrical conductivity was measured using four-probe method between liquid nitrogen temperature and room temperature. ESR spectra are recorded with *JEOL* TE-200 spectrometer equipped with *Oxford* ESR910 continuous-flow helium cryostat. Static magnetic susceptibilities were measured for single-crystalline oriented samples, using Quantum-Design MPMS-5 SQUID magnetometer. The energy band structures of the

salts is calculated based on the tight-binding approximation adopting the extended Hückel Hamiltonian.¹¹ Coefficients for the Slater atomic orbitals were taken from Ref. 8.

RESULTS AND DISCUSSION

C_1 TET-TTF·MX₄ (M = Fe, Ga; X = Cl, Br)

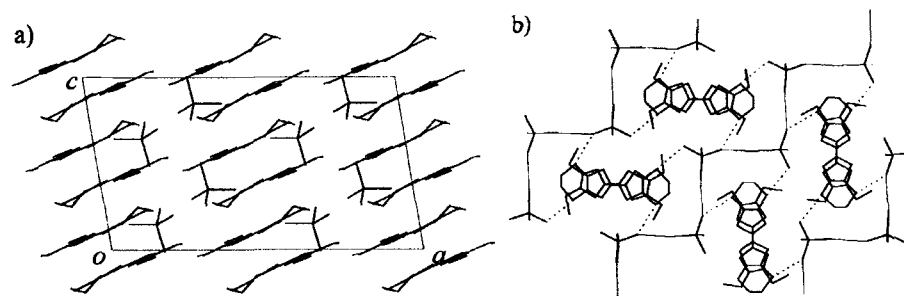


FIGURE 1. Crystal structure of C_1 TET-TTF·FeBr₄ viewed (a) along the b -axis and (b) perpendicular to the $(10\bar{1})$ plane. Close intermolecular contacts are indicated in (b) with thin solid lines (anion – anion) and dashed lines (anion – donor).

These salts crystallize in monoclinic space group $C2/c$ and isostructural to each other. FIGURE 1(a) shows the unit cell of C_1 TET-TTF·FeBr₄ viewed along the b -axis. The two donor molecules form a head-to-tail dimer, which are stacked along the c -axis. The transfer integral between two dimers along this direction (4 meV) is negligibly smaller than the intradimer one (0.35 eV), showing the strong dimerization along the columns. No close side-by-side S··S contacts between the donor molecules exists, as a result of steric hindrance caused by the thiomethyl groups which are bent outwards. These structural features and 1:1 stoichiometry lead to the poor conductivity of the salt ($\sigma_{RT} = 2 \times 10^{-7} \text{ Scm}^{-1}$, $E_A = 0.43 \text{ eV}$). The counter anions form zigzag chains through short X··X contacts (thin solid lines in FIGURE 1(b)), whose distances (X = Cl: 3.67, X = Br: 3.80 Å) are close to the twice of the van der Waals radii (Cl··Cl: 3.50, Br··Br: 3.70 Å).¹² Since the interchain X··X distance along the c -axis (X = Cl: 4.48, X = Br: 4.23 Å) are more longer than the corresponding van der Waals distances, the exchange interaction between the anion chains through this path are considered to be weak. On the other hand, there are a number of close X··S contacts between the counter anion and the dihydrodithiin ring of the donor (dashed lines), whose distances (X = Cl: 3.45, X = Br: 3.62 Å) are shorter than the sum of van der Waals radii (Cl··S: 3.55, Br··S: 3.65 Å).¹²

Therefore the zigzag anion chain is connected with each other by donor dimers to make a sheet structure.

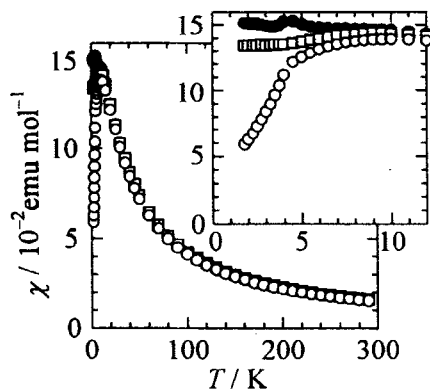


FIGURE 2. Temperature dependence of the magnetic susceptibility of $C_1TET\cdot TTF\cdot FeBr_4$ (\circ : $H \parallel a$, \bullet : $H \parallel b$, \square : $H \parallel c$).

FIGURE 2 shows the magnetic susceptibility of the $FeBr_4$ salt, after the subtraction of the core diamagnetic contribution. The susceptibility obeys the Curie-Weiss law with the antiferromagnetic Weiss temperature of $\Theta = -6.5$ K and -16 K for $FeCl_4$ and $FeBr_4$ salts, respectively. The Curie constants ($X = Cl$: 4.41 , $X = Br$: 4.64 $emu\ K\ mol^{-1}$) show that the main contribution to the susceptibility is the spins on the high-spin $FeBr_4^-$ ion ($s = 5/2$, $C = 4.51$ $emu\ K\ mol^{-1}$). The contribution of the donor spin ($s = 1/2$) is rather well discussed from the results of the ESR measurements: The ESR spectrum for the $GaBr_4$ salt shows the narrow signal ($g = 2.007$, $\Delta H = 1$ mT) assigned to the donor cation radicals thermally excited to the triplet state. For the $FeBr_4$ salt, however, only one broad signal ($g = 2.03$, $\Delta H = 100$ mT) is observed, which is the weighted average of the donor and the anion signals, as a result of the exchange interaction between the counter anion and the donor. For the $FeBr_4$ salt, the peak of the magnetic susceptibility accompanied by the appearance of anisotropy is observed around 9 K (inset of FIGURE 2), then the antiferromagnetic transition takes place at $T_N = 4$ K, with the spin easy axis oriented approximately along the a -axis. For describing the magnetic interaction of this system, the participation of the donor singlet pair is indispensable: If only the nearest neighbor exchange path along the zigzag anion chain ($Fe-X\cdots X-Fe$) is taken into account, the Néel temperature and the absolute value of the Weiss constant should coincide under the molecular field approximation. In practice, the Néel temperature (4 K) is remarkably suppressed compared with the Weiss constant (-16 K), suggesting the existence of the $Fe-X\cdots(donor)_2\cdots X-Fe$ exchange path as a second-nearest neighbor antiferromagnetic

interaction, which works to frustrate the Fe^{3+} spins to diminish the Néel temperature. This interaction also connects the adjacent anion chains, which lead to the long-range ordering of the anion spins below the transition temperature. Although the difference in the $\text{X}\cdots\text{X}$ and $\text{X}\cdots\text{S}$ distances between FeCl_4 and FeBr_4 salt is reasonably explained from the difference in their van der Waals radii, the magnitudes of the exchange interactions are remarkably different. This can be understood as the difference in the polarizability of the anions; the magnetic orbitals of the FeBr_4^- anion are more delocalized to the ligands than in the case of FeCl_4^- anion, hence the intermolecular exchange interaction of the FeBr_4 salt is stronger than the FeCl_4 salt.

$[\text{Ni}(\text{dddt})_2]_3(\text{MX}_4)_2$ ($\text{M} = \text{Fe, Ga}$; $\text{X} = \text{Cl, Br}$)

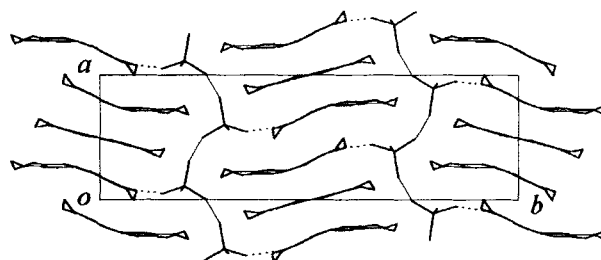


FIGURE 3. Crystal structure of $[\text{Ni}(\text{dddt})_2]_3(\text{FeBr}_4)_2$ viewed along the c -axis.

Close intermolecular contacts are indicated with thin solid lines (anion – anion) and dashed lines (anion – donor).

These isostructural salts crystallize in monoclinic space group $P2_1/n$ and have stoichiometry of 3:2 which is commonly observed in the $\text{Ni}(\text{dddt})_2$ salts.¹³ FIGURE 3 shows the unit cell of $[\text{Ni}(\text{dddt})_2]_3(\text{FeBr}_4)_2$ viewed along the c -axis. Three donor molecules are stacked along the a -axis to form a $\text{A-B-}\bar{\text{A}}$ trimer ($\bar{\text{A}}$ is related to A by inversion symmetry), with the angle of ca. 25° between the long axes of molecules A and B . While molecule B lies on the inversion center and almost planar, the molecules A and $\bar{\text{A}}$ are significantly bent due to the steric effect. The FeX_4^- anions form chains along the c -axis through $\text{X}\cdots\text{X}$ contacts (perpendicular to the figure; distances: Cl : $3.92(2)$, Br : $3.872(3)\text{\AA}$), then these chains are connected to each other by other $\text{X}\cdots\text{X}$ contacts along the a -axis (dashed lines; distances: Cl : $4.09(2)\text{\AA}$, Br : $4.070(4)\text{\AA}$) to make two-dimensional corrugated sheets. These intermolecular distances between halogen atoms are longer than the twice of the van der Waals radii ($\text{Cl}\cdots\text{Cl}$: 3.52 , $\text{Br}\cdots\text{Br}$: 3.70\AA),¹² whereas the $\text{X}\cdots\text{S}$ contacts between the six-membered ring of the donor and the anion (thin solid lines; distance: Cl : $3.48(1)\text{\AA}$, Br : $3.519(5)\text{\AA}$) are significantly close (van der

Waals sum: Cl...S: 3.55, Br...S: 3.65 Å).¹² Thus the existence of the π - d interaction between the donor unit and the magnetic counter anion is expected also for these salts.

On the ESR spectra the FeBr₄ salt gives a single broad Lorentzian peak at room temperature ($g = 2.1$, $\Delta H = 70$ mT), whereas no signal is observed for the isostructural GaBr₄ salt. The signal for the former salt therefore comes only from the magnetic anion, without the contribution of π -electrons on the donor molecules. This agrees with the result of the DC conductivity measurement showing semiconductive behavior ($\rho_{RT} = 3 \Omega\text{cm}$, $E_A = 0.13$ eV). The absence of the conduction electron is explained by the result of the energy band structure calculation, which shows the energy gap $E_g = 0.06$ eV between the conduction band and the valence band. The electronic system of these salts is therefore characterized as a band insulator with a singlet ground state of the donor trimer.

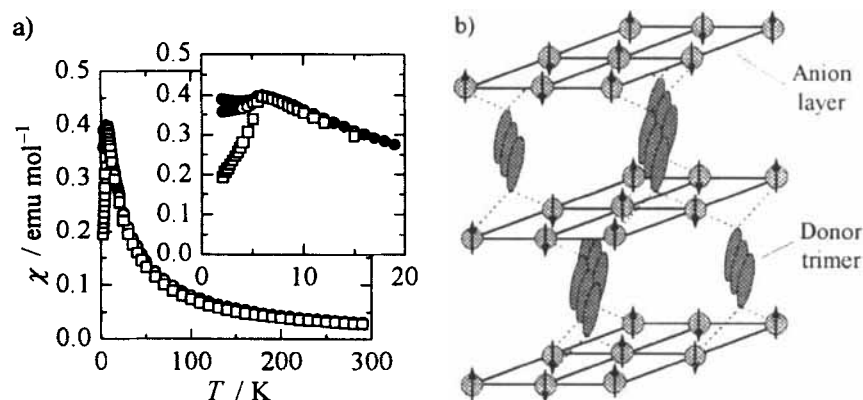


FIGURE 4. (a) Temperature dependence of the magnetic susceptibility of [Ni(dddtt)₂]₃(FeBr₄)₂ (○: $H \parallel a$, ●: $H \parallel b$, □: $H \parallel c$). (b) Schematic diagram of the magnetic structure of [Ni(dddtt)₂]₃(FeBr₄)₂ in the antiferromagnetic phase.

The magnetic susceptibility of these salts obeys the Curie-Weiss law with Weiss temperature $\Theta = -4.7\text{K}$ ($X = \text{Cl}$) and -12.5K ($X = \text{Br}$) (FIGURE 4(a)). The absence of peak in the susceptibility curve, which is ascribed to the short-range order due to the low dimensionality, suggests that the exchange path is three-dimensional. For the both salts antiferromagnetic transitions are observed ($T_N = 2.5\text{K}$ ($X = \text{Cl}$), 6.0K ($X = \text{Br}$)), below which the spin easy axis is oriented along the c -axis (inset). Besides the interlayer exchange interaction between the FeX₄[−] anion through the X...X contacts, the superexchange interlayer interaction through Fe-X...[Ni(dddtt)₂]₃...X-Fe should play an essential role in the long range ordering of the magnetic anions: If only the in-plane interactions in the anion sheet are to be considered, the molecular field approximation

would give the equal absolute values of Curie temperature and Néel temperature, and the short-range order hump should also appear, which are quite different from the experimental results. FIGURE 4(b) schematically illustrate the possible magnetic structure of this salt. Since one donor trimer contacts to the neighboring four FeBr_4^- anion, this trimer connects the anion sheets both structurally and magnetically. Thus the Néel temperature (6.0 K) is suppressed compared to the Weiss constant ($\Theta = -12.5$ K).

[M(dddtt)₂]₂M'X₄ (M = Pt, Au; M' = Fe, Ga; X = Cl, Br)

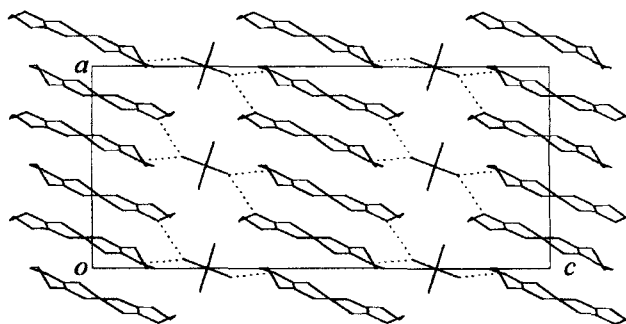


FIGURE 5. Crystal structure of $[\text{Au}(\text{dddtt})_2]_2\text{GaBr}_4$ viewed along the b -axis.

Close intermolecular contacts are indicated with dashed lines.

All salts belong to this group are isostructural to each other, regardless of the metal atoms of the donor (Pt, Au), the anion (Fe, Ga), and the ligand of the anion (Cl, Br). FIGURE 5 shows the unit cell of $[\text{Au}(\text{dddtt})_2]_2\text{GaBr}_4$ viewed along the b -axis. Two donor molecules form a dimer coupled by a weak $\text{Au}\cdots\text{Au}$ contact ($d_{\text{Au}\cdots\text{Au}} = 3.430(2)\text{\AA}$) and, as a result, the molecules are slightly bent from the planarity. The degree of the deviation from the planarity is, however, small compared to $[\text{Pt}(\text{dddtt})_2]_2\text{FeCl}_4$, in which the metal-metal contact is remarkably strong ($d_{\text{Pt}\cdots\text{Pt}} = 2.966(1)\text{\AA}$).¹⁴ The donor dimers are then stacked along the $a + b$ direction to form the donor columns, between which there are a number of $\text{S}\cdots\text{S}$ contacts closer than the twice of the sulfur's van der Waals radius (3.70\AA).¹² The nearest intermolecular $\text{Br}\cdots\text{Br}$ distance is $4.694(8)\text{\AA}$, which is too large for the localized spins on the anions to interact directly each other. On the other hand, there are two close $\text{Br}\cdots\text{S}$ contacts between the donor and the anion as indicated with the dashed line in the FIGURE 5. Since the distance of the closest one ($3.674(9)\text{\AA}$) is close to the sum of van der Waals radii ($\text{Br}\cdots\text{S}$: 3.65\AA),¹² the counter anions are connected through these contacts toward the donor dimer.

These salts show semiconductive behavior with the room temperature conductivity $\sigma_{\text{RT}} = 0.1\text{ Scm}^{-1}$ and the activation energy $E_A = 800\text{K}$. The result of the band structure

calculation shows, however, the existence of the Fermi surfaces and predicts the metallic behavior. Two reasons for this discrepancy are to be considered: The values of the interdimer overlap integrals are larger along the side-by-side direction (b) than the stacking direction ($a + b$), and the resulted one-dimensional Fermi surfaces are unstable against the lattice distortion, resulting in the Peierls state. Another possible explanation is the enhancement of the effective on-site Coulomb repulsion for the dimer as a consequence of the dimerization, which derives the localization of the conduction electrons within the donor columns.

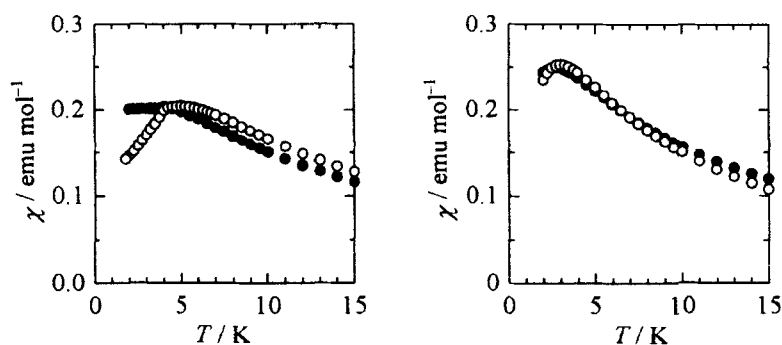


FIGURE 6. Temperature dependence of the magnetic susceptibility of $[\text{Pt}(\text{dddtd})_2]_2\text{FeBr}_4$ (left) and $[\text{Au}(\text{dddtd})_2]_2\text{FeBr}_4$ (right) (O: $H \parallel a$, ●: $H \parallel b$).

The magnetic susceptibility of $[\text{M}(\text{dddtd})_2]_2\text{FeCl}_4$ ($\text{M} = \text{Pt}, \text{Au}$) obeys Curie law regardless of the center metal atom, hence there is little interaction between the magnetic anions in these materials. On the other side, the susceptibility of $[\text{M}(\text{dddtd})_2]\text{FeBr}_4$ show Curie-Weiss behavior ($\text{M} = \text{Pt}$: $\Theta = -5.9 \text{ K}$, $\text{M} = \text{Au}$: $\Theta = -4.6 \text{ K}$) and has a maximum at 4.5 K for Pt and 2.8 K for Au complex (FIGURE 6). For the $\text{Au}(\text{dddtd})_2$ salt, an antiferromagnetic transition takes place at $T_N = 4.5 \text{ K}$, below which the spin easy axis is oriented along the a -axis. Since there is no close contact between the anions, the exchange interaction between two $s = 5/2$ spins ought to be mediated by one $s = 1/2$ spin localized on the dimer unit $[\text{M}(\text{dddtd})_2]_2$ through the path of $\text{Fe}-\text{Br} \cdots [\text{M}(\text{dddtd})_2]_2 \cdots \text{Br}-\text{Fe}$. In this group of the salt, the difference in magnetic behavior between FeCl_4 and FeBr_4 salt can be understood as before, i.e. as the result of higher polarizability of FeBr_4^- anion. Furthermore, the difference between the $\text{Pt}(\text{dddtd})_2$ and $\text{Au}(\text{dddtd})_2$ salt can be explained as follows: According to the extended Hückel calculation, the HOMO of the neutral $[\text{Pt}(\text{dddtd})_2]^0$ complex is in the b_{3u} symmetry, whereas the SOMO of $[\text{Au}(\text{dddtd})_2]^0$ has the b_{1g} symmetry (FIGURE 7). The unpaired electron for the donor dimer is therefore in the b_{3u} and the b_{1g} orbitals for $\text{Pt}(\text{dddtd})_2$ and $\text{Au}(\text{dddtd})_2$ salts, respectively. Since the electron

density on the outer sulfur atom of the b_{3u} orbital is larger than that of the b_{1g} orbital, the unpaired electron spin of the $\text{Pt}(\text{dddt})_2$ dimer is more delocalized to the outer sulfur atom than the $\text{Au}(\text{dddt})_2$ dimer, which makes the transfer integral between $\text{Pt}(\text{dddt})_2$ and the anion more larger than the $\text{Au}(\text{dddt})_2$ case.

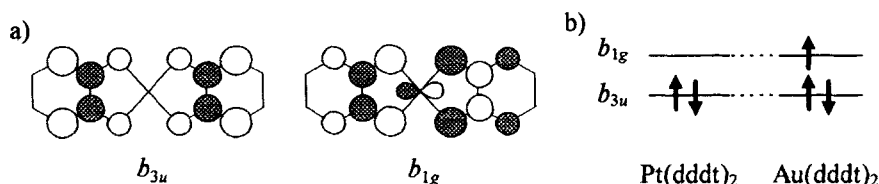


FIGURE 7. Frontier molecular orbitals of $\text{M}(\text{dddt})_2$ ($\text{M} = \text{Pt}, \text{Au}$) (left) and their energy levels for the neutral molecule (right)

SUMMARY

We investigated the crystal structure and the transport and magnetic properties of the three groups of the radical ion salts: $\text{C}_1\text{TET-TTF-FeX}_4$, $[\text{Ni}(\text{dddt})_2]_3(\text{FeX}_4)_2$ and $[\text{Au}(\text{dddt})_2]_2\text{FeX}_4$ ($\text{X} = \text{Cl}, \text{Br}$). Within the crystals of these salts, the counter anions form isolated ($\text{Pt}(\text{dddt})_2$, $\text{Au}(\text{dddt})_2$), chain ($\text{C}_1\text{TET-TTF}$) and sheet structure ($\text{Ni}(\text{dddt})_2$). Their magnetic susceptibilities are, however, three-dimensional, suggesting that the magnetic anions are connected not only through the exchange path of $\text{Fe-X}\cdots\text{X-Fe}$, but also through $\text{Fe-X}\cdots(\text{Donor})_n\cdots\text{X-Fe}$ ($n = 2$ or 3) exchange path to realize the three-dimensionality. The results of the conductivity measurements and the band structure calculation reveal that $\text{C}_1\text{TET-TTF}$ and $\text{Ni}(\text{dddt})_2$ salts are characterized as band insulator, whereas $\text{Pt}(\text{dddt})_2$ and $\text{Au}(\text{dddt})_2$ salts are either in the CDW state or in the Mott insulator phase. All of the FeCl_4 salts shows solely the Curie-Weiss behavior, while the antiferromagnetic transition takes place for all salts when FeBr_4^- is used as a counter anion. These results shows the importance of the high polarizability of the counter anion for the realization of the three-dimensional magnetic interaction in these salts. The difference in the antiferromagnetic transition temperature between $[\text{Pt}(\text{dddt})_2]_2\text{FeBr}_4$ and its gold analogue can be understood as the difference in the symmetry of the orbital in which the localized electron on the donor dimer. For these systems, especially in the case of $[\text{Pt}(\text{dddt})_2]_2\text{FeBr}_4$, the superexchange interaction through the above mentioned path plays an important role in the realization of the long-range order of the magnetic interaction between the magnetic FeBr_4^- anions.

ACKNOWLEDGEMENTS

The present work was partly supported by the Grant-in-Aid for Scientific Research from the Ministry of Education, Science and Culture of Japan.

REFERENCES

1. For example; T. Mallah, C. Hollis, S. Bott, M. Kurmoo, P. Day, M. Allan and R. H. Friend, *J. Chem. Soc. Dalton Trans.*, 859 (1990).
2. J. Yamaura, K. Suzuki, Y. Kaizu, T. Enoki, K. Murata and G. Saito, *J. Phys. Soc. Jpn.*, **65** (1996), in press.
3. T. Enoki, M. Enomoto, M. Enomoto, K. Yamaguchi, N. Yoneyama, J. Yamaura, A. Miyazaki and G. Saito, *Mol. Cryst. Liq. Cryst.*, in press (1996).
4. M.-L. Doublet, E. Canadell, J. P. Pouget, E. B. Yagubskii, J. Ren and M.-H. Wangbo, *Solid State Commun.*, **88**, 699 (1993).
5. A. Kobayashi, T. Udagawa, H. Tomita, T. Naito and H. Kobayashi, *Chem. Lett.*, 2179 (1993).
6. A. Otshuka, Private communications.
7. C. T. Vance, R. D. Bereman, J. Bordner, W. E. Hatfield and J. H. Helms, *Inorg. Chem.*, **24**, 2905 (1985).
8. A. J. Schultz, H.-H. Wang, L. C. Soderholm, T. L. Sifter, J. M. Williams, K. Bechgaard and M.-H. Whangbo, *Inorg. Chem.*, **26**, 3757 (1987).
9. G. M. Sheldrick, *SHELXS86*, Program for crystal structure determination. Univ. of Göttingen, Federal Republic of Germany (1986).
10. G. M. Sheldrick, *SHELXL93*, Program for refinement of crystal structures. Univ. of Göttingen, Federal Republic of Germany (1993).
11. T. Mori, A. Kobayashi, Y. Sasaki, H. Kobayashi, G. Saito and H. Inokuchi, *Bull. Chem. Soc. Jpn.*, **57**, 627-633 (1984).
12. A. Bondi, *J. Phys. Chem.*, **68**, 441 (1964).
13. C. Faulmann, P. Cassoux, E. B. Yagubskii, L. V. Vetoshkina, *New. J. Chem.*, **17**, 385 (1993); E. B. Yagubskii, A. I. Kotov, E. E. Laukhina, A. A. Ignatiev, L. I. Buravov, A. G. Khomenko, V. E. Shklover, S. S. Nagapetyan and Yu. T. Struchkov, *Synth. Metals*, **41-43**, 2515 (1991).
14. O. A. Dyachenko, V. V. Gritsenko, G. V. Shilov, E. E. Laukhina and E. B. Yagubskii, *Synth. Metals*, **58**, 137 (1993).